

A General Method for Constrained Analysis of Fluorescence Anisotropy Decay: Application of the Steady-State Anisotropy

Edward L. Rachofsky,¹ Barnabas Wolf,¹ Carl N. Bialik,¹ J. B. Alexander Ross,¹ and William R. Laws^{1,2}

Received August 7, 1998; accepted April 20, 1999

Time-resolved fluorescence anisotropy is an invaluable method for investigating the internal and rotational dynamics of biomolecules. The range of rotational motions detectable by anisotropy decay is limited by the fluorescence lifetime; typically, a depolarizing motion may be resolved if the associated correlation time is between 0.1 and 10 times the intensity decay lifetime. To extend that range and to improve the recovery of anisotropy decay parameters, a general analytical method has been developed. This procedure utilizes a modification of Lagrange multiplier methods to constrain the values of the iterated kinetic parameters during nonlinear least-squares analysis of anisotropy decay data. The form of the constraint equation is derived from the classic relationship between the decay parameters and the steady-state anisotropy, which can be simply and accurately measured. Application of the constraint to analyses of synthetic data sets increased the accuracy of recovery by decreasing the uncertainty in the iterated parameters. The constraint also enabled the accurate recovery of correlation times that were a factor of 30 greater than the fluorescence lifetime, although it did not improve recovery of correlation times that were much shorter than the lifetime. Using this technique, it should now be possible to characterize the dynamics of larger macromolecules and assemblies than those that can currently be studied by fluorescence anisotropy decay.

KEY WORDS: Fluorescence anisotropy decay; steady-state anisotropy; constrained optimization; Lagrange multiplier method.

INTRODUCTION

Fluorescence anisotropy decay measurements can provide information about both the rotational diffusion and the internal dynamics of a biomolecule [1]. Such measurements depend on the dynamic depolarization of the fluorescence emission due to macromolecular rotations, segmental motions, and local motions of the probe. For a given depolarizing process to be observable, it must

occur on a time scale similar to that of emission. If a rotational correlation time associated with a particular depolarizing process is much shorter than the fluorescence lifetime, the depolarization may be too rapid to be resolved by current instrumentation. If the correlation time is much longer than the lifetime, then the decay of the fluorescence intensity will be complete before a measurable amount of depolarization can take place. Thus, the fluorescence lifetime limits the range of dynamic processes that can be observed accurately by anisotropy decay measurements [2].

A second limitation on the analysis of fluorescence anisotropy data is the statistical cross-correlation between the parameters iterated during data analysis [3]. This

¹ Department of Biochemistry, Mount Sinai School of Medicine, One Gustave L. Levy Place, New York, New York 10029.

² To whom correspondence should be addressed. e-mail: wlaws@smtlink.mssm.edu

correlation arises from the mathematical form of the fitting function, which is usually a product of two sums of exponentials: one sum representing the fluorescence intensity decay kinetics and the second sum the anisotropy decay. Consequently, the uncertainties in the recovered anisotropy parameters can be very large, hampering the assignment of the correct depolarizing mechanism to the observed kinetics. These uncertainties are particularly great in cases where the ratio of the fluorescence lifetime to the rotational correlation time is far from unity, i.e., in the two extreme situations discussed above. Therefore, the range of correlation times that can be determined accurately by fluorescence anisotropy decay has been restricted to within the approximate limits $0.1 \tau \leq \varphi \leq 10 \tau$, where τ is the fluorescence lifetime and φ is the correlation time [2].

To decrease the correlation between iterated parameters, some investigators have attempted to constrain a data analysis by using other types of information. Hydrodynamic calculation of rotational diffusion constants has been used to predict the correlation time(s) due to global rotational motion(s) of a macromolecule [4]. Sedimentation velocity experiments can provide translational diffusion constants for a macromolecule, which can then be used to calculate approximate molecular size, shape, and rotational parameters [4]. Quantum mechanical calculation of the excitation and emission dipoles of the fluorophore can help to predict limiting anisotropies [5]. For systems with multiple fluorophores, anisotropy decay data can be collected as a function of an independent variable, such as excitation or emission wavelength, and then analyzed globally for common rotational parameters [6,7].

This work demonstrates the use of a novel constraint for the analysis of anisotropy decays. This algorithm is a general method that can be used to apply any mathematical relationship between iterated parameters as a constraint on an analysis. In this study, this method has been applied to constraining the anisotropy decay analysis by the value of the steady-state anisotropy. The steady-state anisotropy of a sample can be precisely and accurately measured and is related to the fluorescence intensity and anisotropy decay parameters by a simple formula. This quantity has been applied to constrain anisotropy decay analysis previously [8], but the methods that have been employed can introduce errors into the analysis (see Discussion). The novel algorithm that is presented here is not subject to the limitations of these previous methods. Simulation studies are presented demonstrating that this constraint decreases the uncertainty in the iterated parameters and improves the accuracy of recovery of the parameters used for data generation. This improvement is

particularly dramatic for data sets in which the rotational correlation time is much greater than the fluorescence lifetime.

THEORY

Time-resolved fluorescence data obtained by the method of time-correlated single-photon counting (TCSPC) can be analyzed by several techniques, including nonlinear least squares (NLLS) [9], the method of moments [10], and the Laplace transform [11]. For time-resolved fluorescence data, NLLS has been shown to recover parameters with the maximum likelihood of being correct, provided that the proper theoretical model (fitting function) of the decay kinetics is used [3]. The approach described here is a modification of NLLS.

The objective of NLLS is to minimize χ^2 [12], the weighted sum of the squared residuals for each data point:

$$\chi^2 = \sum_i \frac{1}{\sigma^2(t)} (x_{\text{data}}(t) - x_{\text{fit}}(t))^2 \quad (1)$$

Here $\sigma(t)$ is the statistical weight of $x_{\text{data}}(t)$, which is the value of the data at time t . Time-correlated single-photon counting data inherently obeys Poisson statistics. Therefore, for a large number of counts the distribution of errors is well approximated by a Gaussian, and the statistical weight of each data point is the square root of the number of counts. For TCSPC, the value of $x_{\text{fit}}(t)$ is determined by the choice of the fitting function, the values of the iterated parameters, and the convolution of the analytic fitting function with a measured instrument response function (IRF) to account for the finite time response of the instrumentation.

To constrain an NLLS analysis by any additional mathematical relationship between the iterated parameters, the method of Lagrange multipliers may be applied. This algorithm is similar to previously published methods of restricted least squares, although these techniques have not been applied to fluorescence decay before [13]. A new minimization function, χ_C^2 , is generated by weighted addition of a constraining function to Eq. (1):

$$\chi_C^2 = \chi^2 + \kappa g \quad (2)$$

Here κ is a constant, and g is a constraint function. For constraint by the steady-state anisotropy, g is defined as

$$g = (r_{\text{ss}} - \langle r \rangle)^2 \quad (3)$$

where r_{ss} is the measured value of the steady-state anisotropy and $\langle r \rangle$ is the value of the steady-state anisotropy calculated from the iterated parameters. As the difference

between the calculated and the measured steady-state anisotropies increases, g becomes larger and χ_C^2 becomes increasingly different from χ^2 . The minimum of χ_C^2 with respect to all iterated parameters is equivalent to the minimum of χ^2 subject to the constraint that g is equal to zero, i.e., the value of the steady-state anisotropy calculated from the iterated parameters is equal to the measured value. An alternative description is that this point is the minimum of the function in parameter space defined by the intersection of the χ^2 hypersurface with the curve $g = 0$ [13]. By requiring the minimum to lie on the intersection of these two curves, the constraint decreases the range of acceptable values of each iterated parameter. Therefore, application of the constraint should reduce the uncertainties in the iterated kinetic parameters. If the value of r_{ss} is accurate, then decreasing the parameter uncertainties will also increase the probability of recovering correct values of the kinetic parameters from the analysis.

The minimum value of χ_C^2 is obtained by finding values of the n iterated parameters p_i for which the derivative of χ_C^2 with respect to each is zero:

$$\nabla\chi_C^2 = \nabla(\chi^2 + \kappa g) = \sum_{i=1}^n \left(\frac{\partial\chi^2}{\partial p_i} + \kappa \frac{\partial g}{\partial p_i} \right) = 0 \quad (4)$$

The multiplier κ is analogous to a Lagrange multiplier, in that it weights the contribution of the constraint term to the minimization function. However, here κ must be a *constant multiplier*, whereas a *conventional Lagrange multiplier* is a variable. The invariance of the multiplier is a practical necessity due to the iterative nature of the algorithms used to solve Eq. (4). In such algorithms, the value of each iterated parameter is typically incremented by some δp_i that depends on the partial derivative of χ_C^2 with respect to p_i . If κ were a variable, the derivative of χ_C^2 with respect to κ would be g , which would always be positive. Consequently, χ_C^2 would always decrease as κ decreased, and the value of a variable κ would iterate to zero. This solution is not acceptable, because it effectively removes the constraint.

The value of κ determines the weighting of the constraint term in Eq. (2) and, consequently, the stringency with which the calculated steady-state anisotropy is constrained to approximate the experimentally measured value. The theoretical basis for the choice of the fixed value of κ depends upon the uncertainty in the measured value of r_{ss} [12]. The approximate range of acceptable values of κ may be inferred from the condition that both the decay data and the steady-state anisotropy must contribute significantly to the gradient of χ_C^2 near its minimum. If κ is too small, then the first term in the summation

in Eq. (4) will be much larger than the second term, and the steady-state anisotropy will not apply a significant constraint on the minimization. Alternately, if κ is too large, the first term in the summation will be much smaller than the second term, and the decay data will not be fit well. Numerically, for $\langle r \rangle$ to be constrained to within $\pm \delta r$ of r_{ss} , the value of κ must be sufficient that

$$\sum_{i=1}^n \frac{\partial(\delta r^2)}{\partial p_i} \sim \sum_{i=1}^n \frac{\partial\chi^2}{\partial p_i} \quad (5)$$

when both are evaluated at the minimum of χ_C^2 . The acceptable range δr can be determined from the experimental uncertainty in r_{ss} . It is shown under Results that the performance of the algorithm is insensitive to changes in κ over approximately five orders of magnitude.

Although the Lagrange multiplier method is employed here to constrain by the steady-state anisotropy, this algorithm has more general application. Any independent mathematical relationship between the iterated parameters may be applied as an analysis constraint, simply by changing the expression for g [Eq. (3)]. This relationship may take any algebraic form, provided it has a minimum at which the constraint is satisfied. In fact, any number of constraints may be simultaneously applied, each weighted by an appropriate Lagrange multiplier.

METHODS

Simulations

Fluorescence anisotropy decay data sets were synthesized by a Monte Carlo algorithm as reported previously [14]; the noise generated by the algorithm obeys Poisson statistics and thus is analogous to photon-counting noise. Data were “collected” into 2000 channels with a timing calibration of 22 ps/channel. The IRF was a Gaussian with a full width at half-maximum of 300 ps. For each data set, fluorescence decays were synthesized to simulate data collected with vertically polarized excitation and three emission polarizer angles: the magic angle (M), vertical (V), and horizontal (H) [15]. The formulae describing the decay kinetics at these three positions are provided under Data Analysis, below. Synthesis of the IRF was terminated when 100,000 counts had been collected into the peak channel; those of the M, V, and H fluorescence decays were terminated after 40,000 counts had accumulated in the peak channel. The collection criteria for the simulated data sets were based on those used for actual TCSPC experiments.

Data Analysis

Simulated anisotropy data sets were analyzed by an investigator who was blinded to the values of the kinetic parameters used to generate those data. Analysis was performed by NLLS regression using a reconvolution procedure [16]. The three curves that represented fluorescence decays of a single sample collected at M, V, and H polarizer positions were analyzed to standard formulae:

$$M(t) = \alpha e^{-t/\tau} \quad (6)$$

$$V(t) = \alpha e^{-t/\tau}(1 + 2r(t)) \quad (7)$$

$$H(t) = \alpha e^{-t/\tau}(1 - r(t)) \quad (8)$$

where α is a scaling factor [1]. The function $r(t)$ is the fluorescence anisotropy decay:

$$r(t) = r_0 e^{-t/\varphi} \quad (9)$$

where r_0 is the limiting anisotropy, which is a function of the excitation and emission transition dipoles. The M, V, and H curves for a given data set were analyzed simultaneously by a global procedure [4,17]. Goodness of fit was assessed by the value of χ^2 (or χ_C^2), the weighted residuals, and the autocorrelation function of the residuals.

The value of $\langle r \rangle$ was calculated to four significant figures from the *iterated* parameters by the standard formula [15]:

$$\langle r \rangle = \frac{r_0}{1 + (\tau/\varphi)} \quad (10)$$

Constraint of data analysis by the steady-state anisotropy r_{ss} was performed as described under Theory. For constrained analyses, the value of r_{ss} for each data set was calculated from the *generation* parameters using Eq. (10). The uncertainty of the provided steady-state anisotropy (± 0.0001) was smaller than that of a real experiment by approximately an order of magnitude. This higher precision was employed because these simulations were designed as benchmark tests of the performance of the constraint algorithm. In this way, the performance of the algorithm could be evaluated as a function of several independent variables in the absence of significant numerical round-off errors. The effects of experimental imprecision were subsequently determined by constraining analyses with incorrect values of r_{ss} (see Results).

Parameter Uncertainties and Recovery of Expected Values

Accurate determination of the uncertainties in the parameters iterated during NLLS analysis must account

for the effects of statistical cross-correlation between parameters. A standard procedure for estimating parameter uncertainty that includes the effects of correlation is as follows. Starting from the parameter values corresponding to the minimum of χ^2 , the value of the i th parameter p_i is changed by some δp_i . Now a new minimum of χ^2 is found, allowing all parameters but p_i to vary. This procedure is repeated for a variety of δp_i , so that the rate of increase of χ^2 with increasing δp_i can be determined. The *steepness* of a plot of χ^2 vs δp_i is an estimate of the true uncertainty in p_i , because it represents the rate at which perturbations in this parameter decrease the goodness of fit. A rapid increase in χ^2 indicates that a parameter is precisely determined, while a slow increase is indicative of a large uncertainty in this parameter. By comparing the slope of this curve between analysis protocols (such as with and without the r_{ss} constraint), it is possible to determine which protocol recovers kinetic parameters with greater certainty. This procedure can be repeated for all iterated parameters.

Unfortunately, the above analysis of uncertainties is computationally expensive, because it requires many minimizations to assess even a single parameter uncertainty. Therefore, uncertainties have been determined in this fashion only for a single synthetic data set (see Results), as a benchmark test of the effect of the r_{ss} constraint on the precision of recovered parameters. For all other data sets, uncertainties were estimated by repeating the analysis starting from three different sets of initial guesses of the iterated parameters. The uncertainty in a parameter will be approximately proportional to the scatter in the values recovered from different initial guesses.

It is important to note that the majority of the uncertainty in the kinetic parameters recovered from fluorescence decay data analyzed by NLLS arises from the statistical cross-correlation between iterated parameters [3]. The experimental imprecision in TCSPC data is quite small, since the uncertainty in photon counts increases only as the square root of the number of counts. Consequently, the scatter in the values of parameters recovered from multiple simulations of the same decay is typically far smaller than the uncertainty arising from statistical cross-correlation. Therefore, there is little extra information obtained about parameter uncertainties from repeated synthesis of a decay using the same generation parameters.

For simulated data, it is also possible to evaluate the *accuracy* with which analysis recovers the expected values of the kinetic parameters that were used to generate that data set. The error in a parameter is the difference between the recovered value, p_i^{rec} , and the generation

value, p_i^{gen} . For comparison of multiple analyses or multiple data sets, it is useful to define a *recovery parameter*:

$$R = \prod_{i=1}^n \frac{1}{f_i + 1} \quad (11)$$

where f_i is the fractional error in p_i :

$$f_i = \left| \frac{p_i^{\text{rec}} - p_i^{\text{gen}}}{p_i^{\text{gen}}} \right| \quad (12)$$

The recovery parameter R is a cumulative measure of the deviations between all recovered parameters and their expectation values. The recovery parameter is limited to the range $0 < R \leq 1$, with $R = 1$ indicating exact recovery of all generation parameters, and $R \rightarrow 0$ as $f_i \rightarrow \infty$. The restricted range and simple interpretation of R make it a useful metric for comparing the accuracy of multiple analyses.

RESULTS

Recovery of Kinetic Parameters

To test the ability of the constraint algorithm to improve the recovery of known kinetic parameters, a series of synthetic anisotropy decays was generated using a variety of fluorescence lifetimes, rotational correlation times, and limiting anisotropies. The generation parameters for these data sets are tabulated in Table I. In these data, the ratio of the fluorescence lifetime to the rotational correlation time (τ/ϕ) was varied in small increments from 0.01 to 100. To achieve this large range, lifetimes of 1 and 5 ns were used for $\tau < \phi$ and $\tau > \phi$, respectively. Data sets with intermediate τ/ϕ ratios were generated with both of these lifetimes to ensure that parameter recovery did not depend on the value of the lifetime. For each τ/ϕ ratio, data sets were generated for three limiting anisotropies ($r_0 = 0.05, 0.15, \text{ or } 0.3$). The variation in the values of limiting anisotropies and correlation times was designed to determine the ranges of kinetic parameters for which constraint by the steady-state anisotropy could improve the accuracy of recovery.

Analyses performed without the r_{ss} constraint are summarized in Fig. 1A. As expected, accurate parameter recovery was achieved in the approximate range $0.3 \leq \tau/\phi \leq 10$, with the efficacy of the analysis decreasing drastically beyond either end of this range. The recovery was approximately the same for all limiting anisotropies r_0 , except at very large τ/ϕ . For these very short correlation times, the absolute effects of depolarization on the

Table I. Generation Parameters for Simulated Fluorescence Anisotropy Decays

Data set	$\tau(\text{ns})$	$\phi(\text{ns})$	β	$\langle r \rangle$	τ/ϕ
A	1	100	0.05	0.0495	0.01
B	1	100	0.15	0.1485	0.01
C	1	100	0.30	0.2970	0.01
D	1	30	0.05	0.0484	0.033
E	1	30	0.15	0.1452	0.033
F	1	30	0.30	0.2903	0.033
G	1	10	0.05	0.0455	0.1
H	1	10	0.15	0.1364	0.1
I	1	10	0.30	0.2727	0.1
J	5	50	0.05	0.0455	0.1
K	5	50	0.15	0.1364	0.1
L	5	50	0.30	0.2727	0.1
M	5	15	0.05	0.0375	0.33
N	5	15	0.15	0.1125	0.33
O	5	15	0.30	0.2250	0.33
P	1	1	0.05	0.0250	1
Q	1	1	0.15	0.0750	1
R	1	1	0.30	0.1500	1
S	5	5	0.05	0.0250	1
T	5	5	0.15	0.0750	1
U	5	5	0.30	0.1500	1
V	5	0.5	0.05	0.0045	10
W	5	0.5	0.15	0.0136	10
X	5	0.5	0.30	0.0273	10
Y	5	0.15	0.05	0.0015	33.3
Z	5	0.15	0.15	0.0044	33.3
AA	5	0.15	0.30	0.0087	33.3
BB	5	0.05	0.05	0.0005	100
CC	5	0.05	0.15	0.0015	100
DD	5	0.05	0.30	0.0030	100

V and H decays are numerically very small. Therefore, the declining recovery with decreasing r_0 in this range probably indicates the presence of a critical threshold below which the amplitude of depolarization is too small to observe.

Analyses performed under the r_{ss} constraint are shown in Fig. 1B. Application of the constraint significantly improved parameter recovery for $\tau/\phi < 0.3$ (long correlation times) and resulted in a more modest improvement for $\tau/\phi > 10$ (short correlation times). At both extremes, the recovery deteriorated in an r_0 -dependent fashion.

Further examination of the analyses summarized in Fig. 1 revealed two interesting points. First, the expected value of the fluorescence lifetime τ was successfully recovered to within 0.03 ns for all analyses, regardless of the value of ϕ or the algorithm employed. Therefore, the increases in R observed upon application of the r_{ss} constraint represent more accurate recovery of r_0 and ϕ . Second, the limited efficacy of the constraint at short

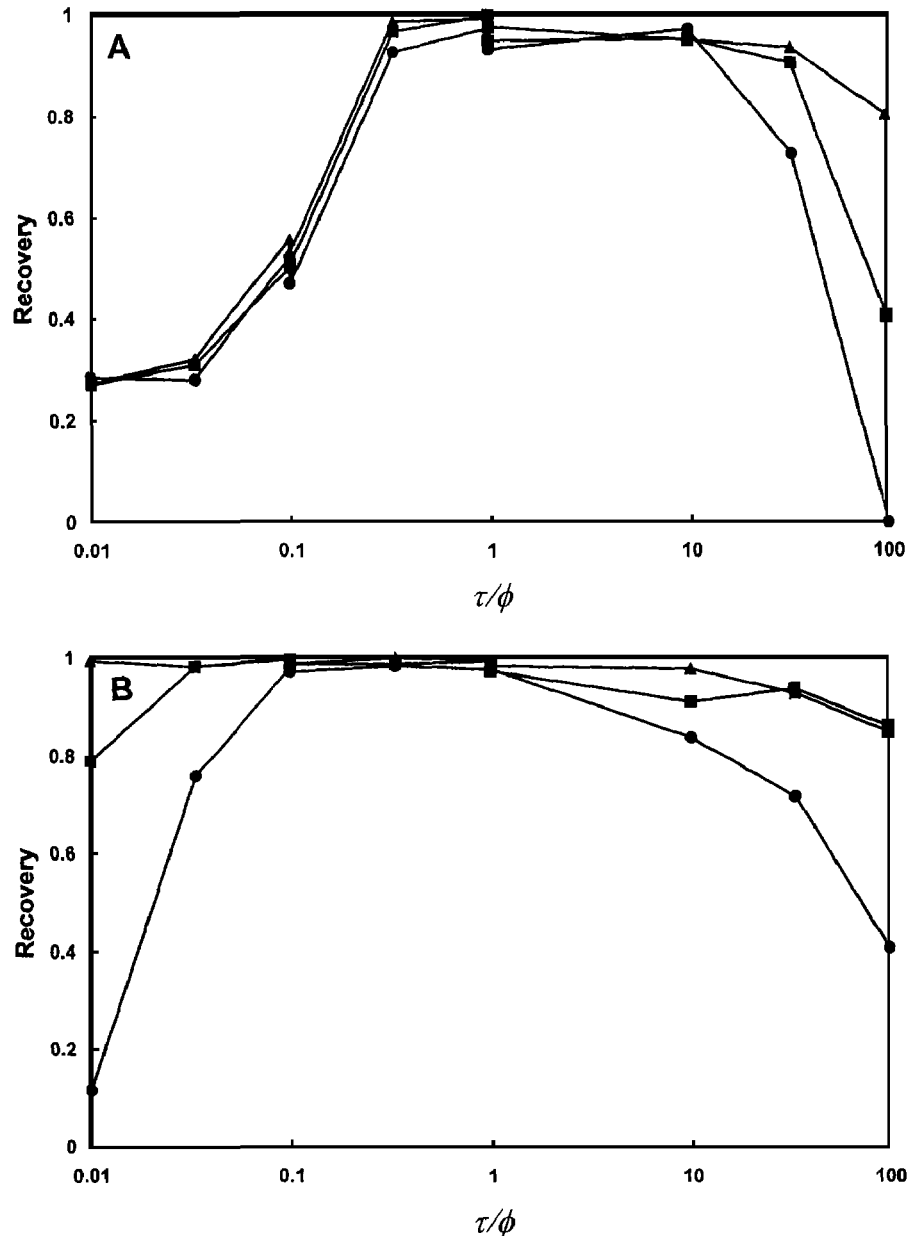


Fig. 1. Recovery of iterated parameters for $r_0 = 0.05$ (\bullet), 0.15 (\blacksquare), and 0.30 (\blacktriangle). (A) Unconstrained analyses; (B) constrained analyses, $\kappa = 10^8$. Lines are drawn only to connect points and do not represent any sort of theoretical fit to the data.

correlation times probably represents uncertainty in the determination of r_{ss} . For these analyses, r_{ss} was accurate to ± 0.0001 , but at the short ϕ limit, this accuracy provided only one or two significant figures. Since realistic experimental uncertainties are of the order of ± 0.003 , the value of r_{ss} cannot be determined to sufficient accuracy to constrain decay analyses for very short correlation times and/or very small limiting anisotropies. Therefore, it is concluded that the r_{ss} constraint improves the accuracy of recovered parameters only in the range $0.01 < \tau/\phi \leq$

0.3 . Nevertheless, this range represents at least an order of magnitude increase in the maximum observable correlation time.

Uncertainty of Recovered Parameters

To test the hypothesis that the r_{ss} constraint decreases the uncertainties in recovered parameters, the effect on the goodness of fit of forcing τ , r_0 , and ϕ away from their optimum values was investigated. A single data set

(E; Table I) was selected for which the r_{ss} constraint significantly increased R . The minimum of χ_C^2 was found while fixing each parameter successively at a series of values $\tau + \delta\tau$, $r_0 + \delta r_0$, and $\varphi + \delta\varphi$, as described under Methods. The results for each of the three parameters were found to be substantively the same for either positive or negative δp_i ; consequently, only absolute values of δp_i are shown. Figure 2A shows that the uncertainty of the recovered fluorescence lifetime did not change upon

application of the r_{ss} constraint. The goodness of fit, represented by χ_C^2 , rapidly decreased with even small deviations from the optimum value of τ . The independence of the uncertainty in τ on the method of anisotropy decay analysis is to be expected, given that the fluorescence lifetime is determined largely from the magic angle decay, which contains no information about depolarizing processes. Figures 2B and C show that the r_{ss} constraint dramatically decreased the uncertainty in r_0 and φ , respec-

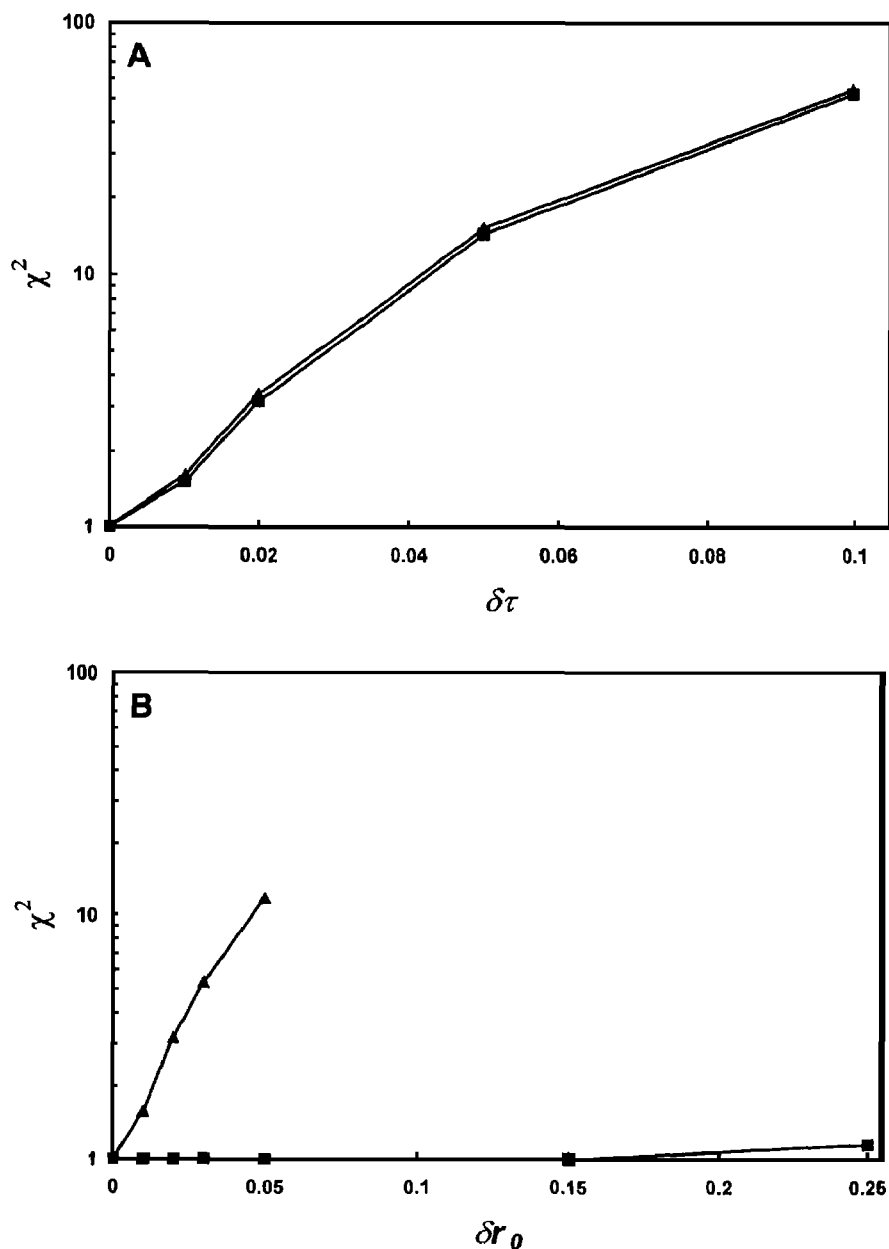


Fig. 2. Parameter uncertainties without (■) and with (▲) constraint ($\kappa = 10^8$), for data set E. For unconstrained analyses, χ^2 is plotted; for constrained analyses, χ_C^2 is plotted. (A) Uncertainty in τ ; (B) uncertainty in r_0 ; (C) uncertainty in φ . Lines are drawn only to connect points and do not represent any sort of theoretical fit to the data.

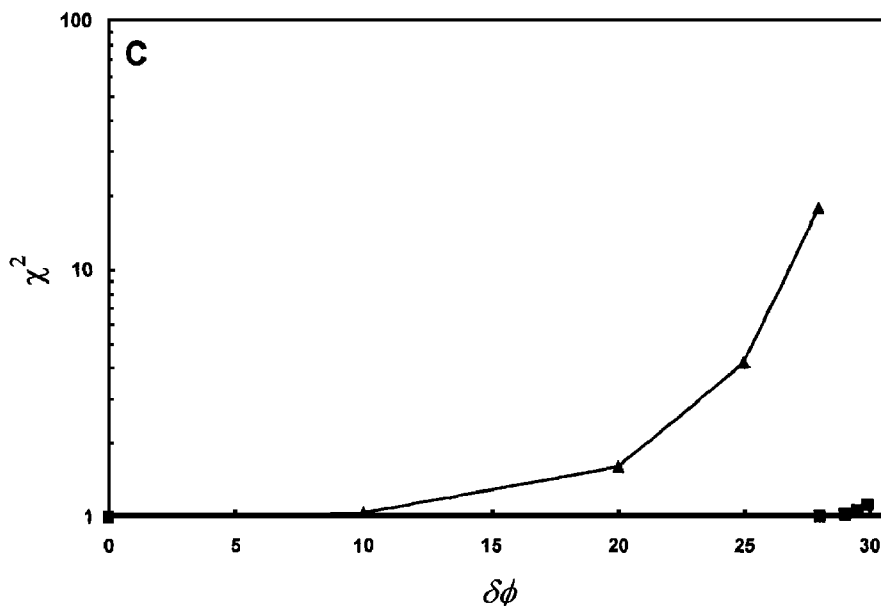


Fig. 2. (Continued).

tively. In the absence of constraint, the values of these parameters may be doubled with little reduction in the goodness of fit. In the constrained analysis, the uncertainties in these parameters are significantly smaller, although they are still much larger than that of the fluorescence lifetime. In both constrained and unconstrained analysis, forced perturbation of φ from its optimum value always resulted in a compensatory change in r_0 , and vice versa. These compensatory changes represent the statistical cross-correlation between the two parameters. However, the r_{ss} constraint significantly decreased the amplitude of the compensatory change, implying that the parameter correlation was weakened. Therefore, it is concluded that application of the r_{ss} constraint decreased the uncertainty of recovered kinetic parameters in the regime where $\varphi \gg \tau$. This type of error analysis was not performed for the cases $\varphi \approx \tau$ or $\varphi \ll \tau$, because the r_{ss} constraint did not increase the accuracy of parameter recovery in these circumstances.

Effects of an Incorrect Constraint

In each of the above simulation studies, the value of r_{ss} used in evaluating the effects of constraint on the recovery and the uncertainty of kinetic parameters was the value calculated from the generation parameters. However, in a real experiment, the determination of r_{ss} is subject to some degree of experimental imprecision. Therefore, the effects of applying an incorrect r_{ss} as an analysis constraint were investigated. Two data sets were selected for this analysis: one (T; Table I) for which

$\varphi = \tau$ and one (E; Table I.) for which $\varphi \gg \tau$. Thus, the effect of an incorrect constraint could be evaluated both under conditions in which a correct constraint improved parameter recovery and those in which it did not. The results are shown in Fig. 3. For both data sets, increasing δr_{ss} resulted in a decrease in the recovery parameter R . The effects of positive and negative δr_{ss} were approximately the same. However, a relatively large δr_{ss} was required to diminish significantly the accuracy of recovered parameters. Both data sets had acceptable R values (>0.9), even for conservative estimates of experimental imprecision ($\delta r_{ss} \leq \pm 0.01$). It is concluded that the improvement in parameter recovery due to the constraint is essentially insensitive to realistic experimental uncertainty in the steady-state anisotropy.

The effect of an incorrect constraint on χ_C^2 was dramatically different for the two data sets. As Fig. 3 demonstrates, there was a much larger increase in χ_C^2 with increasing δr_{ss} for $\varphi = \tau$ than for $\varphi \gg \tau$. This very different behavior is the consequence of the much greater uncertainty in the longer correlation time. When $\varphi = \tau$, the value of φ is very precisely determined from the decay, and consequently any error in r_{ss} results in a decrease in the goodness of fit. When $\varphi \gg \tau$, the value of φ is poorly determined from the decay, and a wide range of values of r_{ss} is consistent with a good fit. Therefore, an incorrect constraint will not result in a statistically unacceptable fit for the case $\varphi \gg \tau$. Because the true kinetic parameters are unknown for experimental data, it will be impossible to detect a bad constraint from the decay analysis when $\varphi \gg \tau$. However, a data set for

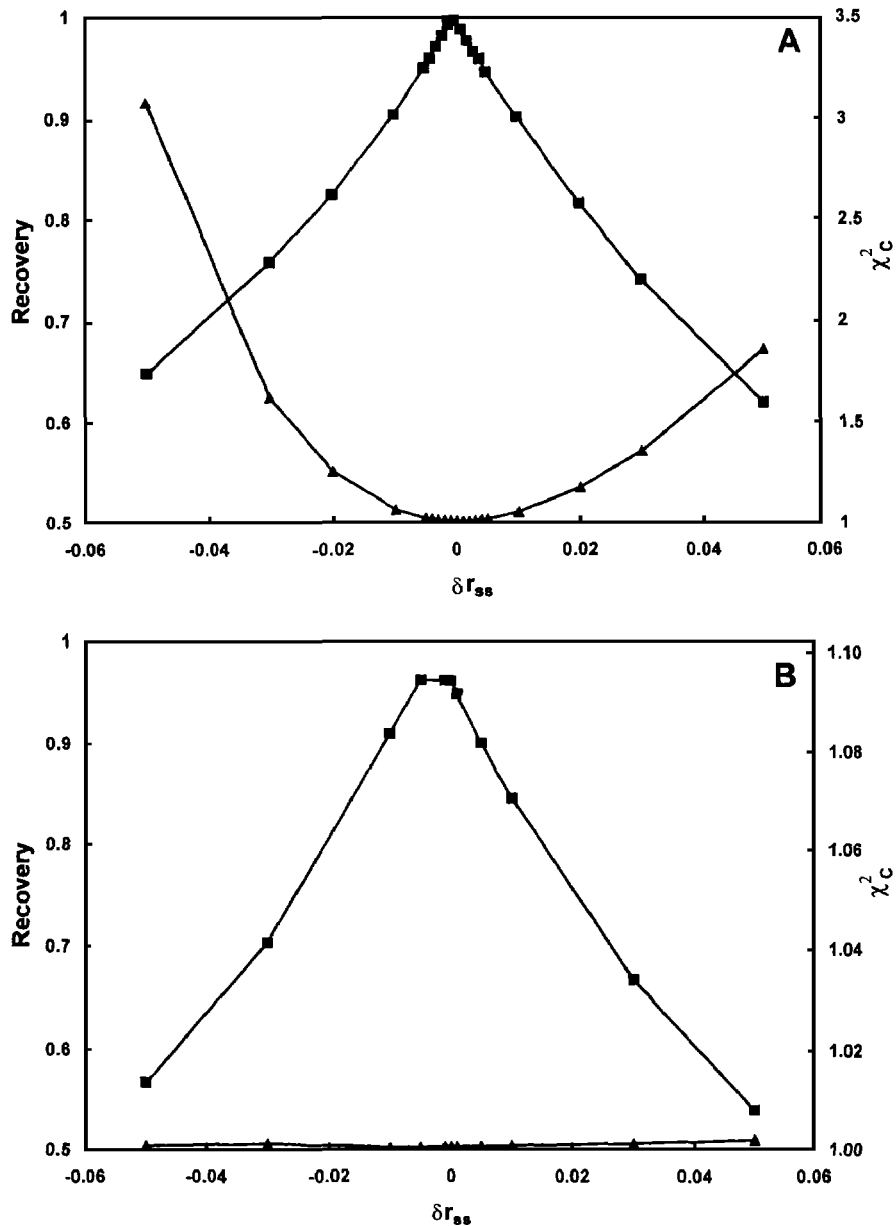


Fig. 3. Recovery of iterated parameters (■) and χ^2 (▲) with constraint by incorrect values of r_{ss} ($\kappa = 10^8$). (A) Data set T, $\tau = \phi$; (B) data set E, $\tau \ll \phi$. Lines are drawn only to connect points and do not represent any sort of theoretical fit to the data.

which $\phi \approx \tau$ may serve as an adequate control for the accuracy of the r_{ss} measurement, since in this case an incorrect constraint should reduce the goodness of fit noticeably.

Choice of Lagrange Multiplier

As stated under Theory, the value of κ should be determined by the uncertainty in r_{ss} . In practice, however, other values may be acceptable. Criteria suggesting a range of acceptable values of κ [Eq. (5)] depend on the

partial derivatives of χ^2 and g with respect to the iterated parameters p_i . However, it is not generally convenient to examine these derivatives during data analysis. Therefore, it would be practical to determine the acceptable range of κ empirically based on the analysis of simulated data. This analysis was performed for a single data set (E; Table I) for which application of the constraint with $\kappa = 10^8$ (see Fig. 1) had significantly improved parameter recovery. Figure 4 shows the effects of changing κ on R and χ^2_C for this data set. The effect of the r_{ss} constraint depended significantly on the value of κ . For $\kappa \leq 10^3$,

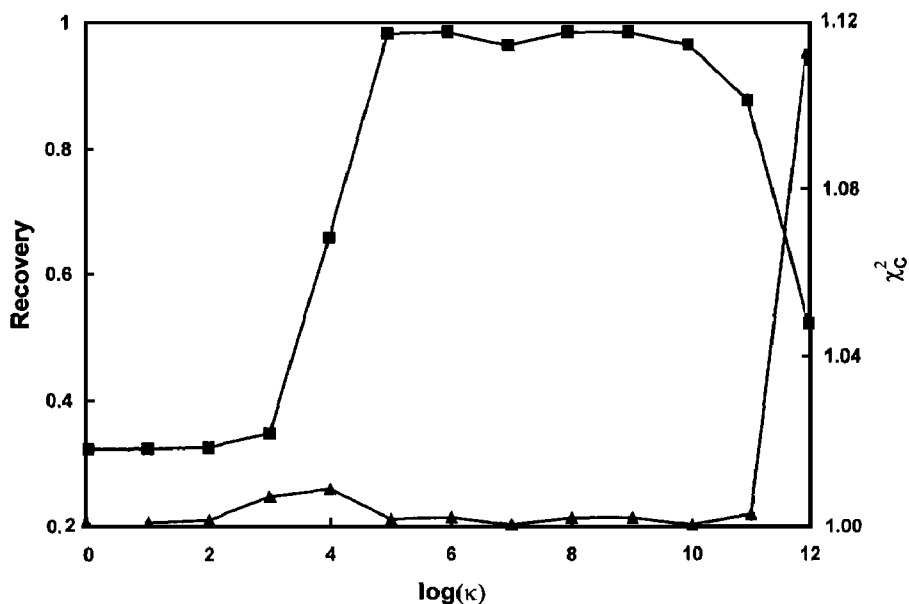


Fig. 4. Recovery of iterated parameters (■) and χ_C^2 (▲) vs the Lagrange multiplier for data set E. Lines are drawn only to connect points and do not represent any sort of theoretical fit to the data.

R was small, indicating that the iterated parameters were not well constrained, and the steady-state anisotropy, $\langle r \rangle$, calculated from the recovered parameters was not equal to r_{ss} (data not shown). As κ was increased to 10^5 , the constraint on the iterated parameters gradually increased, as evidenced by the increase in R . The full effect of the constraint was manifested for $10^5 \leq \kappa \leq 10^9$, and $\langle r \rangle$ was maintained equal to r_{ss} . For $\kappa > 10^9$, the accuracy of the recovered parameters decreased again. Moreover, at these high values of the Lagrange multiplier, the goodness of fit deteriorated, as can be seen from the increase in χ_C^2 in Fig. 4. These results are consistent with the expectation that κ must fall within a certain range to constrain the data properly. If κ is too small, the steady-state anisotropy does not constrain the analysis; if it is too large, the decay curve is not fit adequately.

The broad range of values—five orders of magnitude—of the Lagrange multiplier that provide both good fits and accurate parameter recovery suggests that a default value of κ may be chosen confidently from the middle of this range for subsequent analyses. A default value of $\kappa = 10^8$ is suggested. Moreover, these results suggest simple criteria for changing κ . If the constraint does not maintain $\langle r \rangle$ equal to r_{ss} , then κ should be increased. If application of the constraint significantly increases χ_C^2 , then κ should be decreased. It should be noted that an unacceptable χ_C^2 or $\langle r \rangle$ may also indicate that either the experimental value of r_{ss} or the kinetic model used in data analysis is incorrect. These problems

are indicated if changing the value of κ over several orders of magnitude does not provide acceptable analyses.

DISCUSSION

Fluorescence anisotropy decay measurements are practically limited by the statistical cross-correlation between iterated kinetic parameters during data analysis. We have developed a novel method of constraining the iterated parameters in an NLLS analysis of fluorescence anisotropy decay and employed it to constrain analyses by the steady-state anisotropy. This method utilizes the mathematical relationship between the kinetic parameters and the steady-state anisotropy to restrict the search for a minimum in parameter space. Application of this constraint to the analysis of synthetic data reduced the uncertainty in the iterated parameters and increased the accuracy of parameter recovery. This algorithm increased by approximately an order of magnitude (from $\sim 3\tau$ to $\geq 30\tau$) the maximum rotational correlation time that could be resolved from simulated anisotropy decay data. This advance should enable the measurement of the rotational diffusion of larger macromolecules and assemblies than formerly was possible. Experiments to test the utility of constrained analysis on the anisotropy decay of proteins and other biomolecules are currently in progress.

Three other algorithms have previously been developed to apply the steady-state anisotropy as a constraint

on anisotropy decay analysis [8]. These methods each rely on the fact that the integrals of the decay curves measured at vertical and horizontal emission polarizations can be related to the steady-state anisotropy via the familiar definition

$$\langle r \rangle = \frac{\int_{t=0}^{\infty} (V - H) dt}{\int_{t=0}^{\infty} (V + 2H) dt} \quad (13)$$

in which it is assumed that the steady-state fluorescence intensity at each polarization is equal to the integral of the respective decay. In the first algorithm, the vertical and horizontal decays are collected for equal times, and the steady-state anisotropy is calculated directly from the integrals of these curves [8]. A problem arises with this approach because the total photon flux is not the same at the two polarizations, and therefore the vertical and horizontal decays will not be collected to equal counts. Because the uncertainty in the sum counts at each time point is equal to the square root of the number of counts, the uncertainties in the vertical and horizontal decay curves are also unequal. Consequently, the two curves are not equally weighted in the calculation of χ^2 [Eq. (1)]. However, the two decay curves should be weighted equally in the analysis, because each contains independent and equally significant information. Unequal weighting may change the values of iterated parameters that maximize the goodness of fit and, thus, decrease the accuracy of the recovered parameters.

In the second procedure, the M, V, and H curves are collected to equal peak counts, and the latter two are weighted to scale the ratio of their amplitudes to the theoretically expected value [18]. The ratio of the scalars which weight the vertical and horizontal decays is fixed according to the measured value of the steady-state anisotropy. The problem with this approach is that the scalars do not directly constrain the kinetic parameters describing the anisotropy decay but, instead, determine the amplitudes of the convolved data curves. Therefore, the ratio of the V and H scalars is not necessarily related to the steady-state anisotropy in a simple fashion, because convolution may alter the relative integrals of the two curves.

In the third procedure, the M, V, and H decays are collected to equal peak counts, and the ratio of V and H scalars is estimated to be equal to the ratio of the intensities of these two curves at some time long after excitation [19]. This method is based on the presumption that the emission will be completely depolarized before the intensity becomes undetectable, so that at the tail of the decay curves the amplitudes of V and H are equal. This algo-

rithm is statistically flawed, because it relies on matching the poorly determined tails of the decay curves. It is also inapplicable to the case of $\varphi \geq \tau$.

The algorithm that is presented here avoids the difficulties involved in multiplying convolved data curves or in tail matching, because it directly restricts the iterated kinetic parameters that describe the anisotropy decay. This procedure does not create unequal photon counting uncertainties for M, V, and H decays and does not introduce convolution artifacts into the constraint equation. Unlike the earlier methods, the restriction that is applied to the iterated parameters only depends on the anisotropy decay model.

It has been suggested previously that fluorescence correlation spectroscopy (FCS) could be employed to measure rotational motions occurring much slower than the decay of the excited state [20]. This approach was initially demonstrated for bovine carbonic anhydrase B, for which the mean rotational correlation time is approximately 10 times the lifetime of the extrinsic fluorescent probe employed [21]. The limitations of this FCS method are the use of flow conditions that would perturb the rotational motion of asymmetric molecules, the need for a large sample volume, long data collection times, extensive data manipulation, and the ability to resolve only the harmonic mean rotational correlation time. The steady-state anisotropy constraint method presented here to assist in extracting long correlation times from TCSPC data avoids these complications.

The application of the Lagrange multiplier algorithm to the analysis of fluorescence anisotropy decay is not limited to constraint by the steady-state anisotropy. Any additional information that restricts one or more kinetic parameters can be incorporated into an analysis by use of a suitable constraint equation and fixed Lagrange multiplier. For instance, if a fluorophore is subject to multiple depolarizing motions, the anisotropy decay [Eq. (9)] is multiexponential, and the limiting anisotropy r_0 is the sum of the preexponential factors. The value of r_0 could be determined independently (e.g., by measurement in a highly viscous solvent) and applied as a constraint on the sum of those preexponential factors. [It would also be possible to constrain this type of analysis by iterating all preexponential factors but one and calculating the final one by subtraction of the others from r_0 . However, the current algorithm is a more general method because it is independent of any other constraint placed on the iterated parameters.] Another possible application of the current constraint method would be to do global analysis of fluorescence decays. For example, consider macromolecules that undergo complex assembly interactions. Decays collected at different macromolecular concentrations could

be analyzed globally, with the amplitudes associated with various species constrained to follow the predictions of a thermodynamic model of assembly stoichiometry and energetics.

In conclusion, the results of any relevant physical measurement or a particular relationship between parameters may be applied as a constraint on the analysis by the Lagrange multiplier method. This information should enable more confident determination of kinetic models for fluorescence decay and, consequently, improved understanding of macromolecular dynamics.

ACKNOWLEDGMENTS

The authors wish to thank Dr. Carol Bodian and Dr. Istvan Sugar for helpful discussions and Ms. Elena Rusinova for expert assistance in generating figures. This work was supported in part by NIH Grants GM39750, HL29019, and CA63317.

REFERENCES

1. M. Badea and L. Brand (1979) *Methods Enzymol.* **61**, 378–425.
2. Ph. Wahl (1979) *Biophys. Chem.* **10**, 91–104.
3. M. L. Johnson and L. M. Faunt (1992) *Methods Enzymol.* **210**, 1–36.
4. E. Waxman, W. R. Laws, T. M. Laue, Y. Nemerson, and J. B. A. Ross (1993) *Biochemistry* **32**, 3005–3012.
5. E. L. Rachofsky, J. B. A. Ross, M. Krauss, and R. Osman (1998) *Acta Phys. Pol. A* **94**, 735–748.
6. J. M. Beechem, J. R. Knutson, J. B. A. Ross, B. W. Turner, and L. Brand (1983) *Biochemistry* **22**, 6054–6058.
7. J. R. Knutson, J. M. Beechem, and L. Brand (1983) *Chem. Phys. Lett.* **102**, 501–507.
8. R. E. Dale (1983) in R. B. Cundall and R. E. Dale (Eds.), *Time-Resolved Fluorescence Spectroscopy in Biochemistry and Biology*, Plenum Press, New York.
9. J. H. Easter, R. P. DeToma, and L. Brand (1976) *Biophys. J.* **16**, 571–583.
10. I. Isenberg and R. D. Dyson (1969) *Biophys. J.* **9**, 1337–1350.
11. A. Gafni, R. L. Modlin, and L. Brand (1975) *Biophys. J.* **15**, 263–280.
12. P. R. Bevington (1969) *Data Reduction and Error Analysis for the Physical Sciences*, McGraw–Hill, New York.
13. R. Fletcher (1981) *Practical Methods of Optimization*, John Wiley & Sons, Chichester.
14. F. N. Chowdhury, Z. S. Kolber, and M. D. Barkley (1991) *Rev. Sci. Instrum.* **62**, 47–52.
15. J. R. Lakowicz (1983) *Principles of Fluorescence Spectroscopy*, Plenum Press, New York.
16. A. Grinvald and I. Z. Steinberg (1974) *Anal. Biochem.* **59**, 583–598.
17. A. J. Cross and G. R. Fleming (1984) *Biophys. J.* **46**, 45–56.
18. W. E. Blumberg, R. E. Dale, J. Eisinger, and D. Zuckerman (1974) *Biopolymers* **13**, 1607–1620.
19. J. Vanderkooi, S. Fischkoff, B. Chance, and R. A. Cooper (1974) *Biochemistry* **13**, 1589–1595.
20. M. Ehrenberg and R. Rigler (1974) *Chem. Phys.* **4**, 390–401.
21. P. Kask, P. Piksarv, Ü. Mets, M. Pooga, and E. Lippmaa (1987) *Eur. Biophys. J.* **14**, 257–261.